Effect of stressing on the isotopic composition of plant-emitted carbon monoxide

Sem Vijverberg

June 5, 2015

Coaches:
R.A. Mantel J.H.R. Lambers

Final paper
The Hague University

Contents

Abstract

The isotopic composition of the CO emitted by a plant due to photo- and thermal degradation is determined for the first time, and different circumstances were tested (*living leaf, stressed leaf and cut off / senescent leaf*). This was done by trapping the plant-emitted CO inside a transparent plastic bag. The molar concentration and stable isotopes values (δ^{13}C and δ^{18}O) were measured from air samples before and after a certain time interval., and from these the isotopic composition of the added CO could be calculated. However, the bag enclosing the branch emitted CO and interfered with the tests, thus a correction had to be implemented.

Comparing the averaged δ^{13}C(CO) values of the three tested situations (*living leaf, stressed leaf and cut off / senescent leaf*, they matched pretty well ($-35,4$ to $-36,5$‰), indicating that the CO-formation proces was not substantially affected by the different situations as mentioned above. However, the individual δ^{13}C values were quite spread. The average over all δ^{13}C values (n=18) was $-35,6$‰ with a standard deviation of $\pm 5,7$‰. The δ^{18}O(CO) values were less variable within each situation, yet comparing the different situations, the averaged values varied quite widely. The δ^{18}O(CO) values of the CO emitted by the living (unstressed) leaf were significantly more enriched in the heavy isotope (^{18}O) compared to the stressed and cut off situations. This could indicate that a different origin or reaction pathway of the oxygen atom arises when a plant is stressed and senescent. Moreover, the δ^{18}O values of CO emitted by the cut off branch varied widely as function of time since it was cut, also indicating that plant liquids could play a role in the formation of CO.

Preface

This research was performed for my bachelor of applied physics graduation assignment, conducted at the Institute for Marine and Atmospheric Research Utrecht (IMAU) of the Utrecht University. The institute contributes to the fundamental science of the ocean, atmosphere and cryosphere being divided in 5 different research groups. I was hoping for a research topic that would combine physics and climate science, and i'm really glad this opportunity, to contribute to the Atmospheric Physics and Chemistry group, was given to me. I would like to thank Arnold van Dijk, who has provided the analysis of δ^{13}C in bulk plant material and Dr. Elena Popa, who supervised and guided me in a great way, throughout the entire project.

1 Introduction

Although carbon monoxide is a trace gas in the atmosphere and has a negligible direct effect on the radiative balance, it has important implications for the climate through indirect effects, and for the atmospheric chemistry (Daniel and Solomon, 1998; Huang et al., 2013; Shindell et al., 2009). Multiple effects arise due to CO's interplay with the OH radical. OH oxidises approximately 85% of atmospheric CO to CO_2 (Prinn, 2003; Bergamaschi et al., 2000b; Lu and Khalil, 1993), thereby CO is reacting with 75% of all atmospheric OH (Thompson, 1992). Luckily, the OH is being regenerated, depending on NOx concentration, but there is a net loss (Lu and Khalil, 1993). The OH radical is an important control for the removal of many pollutants and is also the main sink for CH_4, a strong greenhouse gas. CO is therefore competing with CH_4 to react with OH, influencing the lifetime of CH_4, and other pollutants (Khalil and Rasmussen, 1985; Wang and Prinn, 1999; Lu and Khalil, 1993). Moreover, due to CO's claim on OH, it also plays an important role on the formation of sulfate aerosols (Wang and Prinn, 1999; Shindell et al., 2009), and it (directly and indirectly) contributes to the formation of ozone (Fishman and Crutzen, 1978).

Atmospheric CO has a wide variety of sources, CH_4 oxidization, fossil fuel, biomass burning and non-methane hydrocarbon (NMHC) oxidation, presenting the main contributors (Park, 2010). Due to large temporal and spatial differences in emissions, the CO budget is difficult to model (Wang et al., 2012; Park et al., 2015; Conny, 1998). Instead of using solely CO mixing ratios to reconstruct the different source strengths, the complementary information of the stable isotopes can be used. Different sources emit CO with a specific isotopic composition, which is often called the source signature (Brenninkmeijer, 2009). The individual isotopomers ^{13}C and ^{18}O can render an extra constrain on the models (Manning et al., 1997). This approach was adopted by Manning et al. (1997); Bergamaschi et al. (2000a) and recently by Park (2010) and Park et al. (2015), and they showed more robust results compared to models incorporating CO mixing ratios only. However, the CO signatures available were only estimated for the main sources, and were deduced indirectly by analysing isotopic composition of ambient atmospheric CO with the corresponding temporal and spatial emission and fractionation rate(s) (Stevens et al., 1972; Stevens and Wagner, 1989; Conny, 1998; Brenninkmeijer et al., 1999, 2003). So far, the isotopic composition of various sources remains uncertain and further analysis of individual source signatures is essential (Brenninkmeijer et al., 2003; Brenninkmeijer, 2009; Bergamaschi et al., 2000a).

Plant foliage is known to emit CO due to photo-degradation. Direct CO emission of senescent leaves were found to be a factor 1.3 to 5.4 times higher compared to living leaves by Tarr et al. (1995), Yonemura et al. (1999) reported a factor 9. The CO emission was found to be strongly reduced in the absence of oxygen (Derendorp et al., 2011). Photo-degradation increases linearly with light intensity (Yonemura et al., 1999; Derendorp et al., 2011) and although the UV-spectrum comprises only a small part of the (energetic) surface radiation spectrum, tests conducted by Bruhn et al. (2013) and Schade and Crutzen (1999) showed

it accounted for, respectively, 50% and 60% of the total CO production. CO can also be produced by thermal degradation (Schade and Crutzen, 1999). It is suggested that thermal and photon energy could be used synergistically to dissociate the chemical bonds, although photo-degradation is responsible for approx. 90% of the plant-emitted CO (Lee et al., 2012). Different biochemical mechanisms responsible for photo-degradation induced carbon fluxes have been proposed, however, they remain unclear (van Asperen et al., 2015). The most recent research suggests there may be multiple mechanisms involved, those requiring O_2 and those who do not. For the anoxic mechanism, Lee et al. (2012) suggests either direct CO formation (without an oxidising proces, directly emitting CO) or that C is oxidised by oxygen species originating from within plant material. Simultaneously, photo-chemically mediated oxidation can occur, using atmospheric O_2 or other reactive oxygen species.

Although the source strength of plant-emitted CO represents only ∼2 to 8% of the global CO budget (Schade and Crutzen, 1999), CO degradation can be more important in remote, unpolluted regions, were vegetation is often abundant (Tarr et al., 1995). Additionally, low NO_x levels are generally observed in such remote regions, which may limit CO production from non-methane hydrocarbons (NMHC) (Tarr et al., 1995), and increase the OH consumption by CO (Lu and Khalil, 1993), potentially further increasing the relative importance of CO emission. Moreover, abiotic photo-degradation was shown to induce a much larger impact on litter decomposition compared to biotic degradation in semi-arid and arid ecosystems(Austin and Vivanco, 2006). Until recently, this was unaccounted for in decomposition models and consequently, mass loss in arid and semi-arid environments were underestimated. However, the updated higher role on mass loss due to photo-degradation in arid systems still does not fully account for the underestimation of mass loss. "Further empirical and modeling studies of interaction between photo-degradation and other abiotic and biotic controls on decomposition are needed" (Brandt et al., 2010).

In this paper, an isotope analysis is performed on plant-emitted CO. Isotopic information could render improvements for CO models and it may elucidate aspects of the proces(ses) involved in photo- and thermal degradation. For the first time, the plant-emitted CO isotopic signature is determined based on direct measurements of the stable isotope values $\delta^{13}C(CO)$ and $\delta^{18}O(CO)$. A branch is enclosed with a plastic bag, the plant-emitted CO is captured in the air tight bag, which already contains ambient air, and subsequently, the added CO induces an isotopic change in the air present in the bag. The plant-emitted CO isotope values are calculated based on the increased mixing ratio and corresponding isotopic change, over a certain time interval. The bag air is sampled at the start and end of a certain time interval, and the isotopic composition of the samples is measured using a gas chromatograph - isotope ratio mass spectrometer (GC-IRMS). Moreover, plant material was collected and prepared for bulk composition analysis of carbon by an external laboratory.

2 Theory

2.1 Definitions and notations

To quantify an amount of molecules, the mole fraction is commonly used, which can be expressed in nmol/mol or parts per bilion (ppb). 1 ppb means that there is 1 CO molecule in a billion other gas molecules. Typical mole fractions of carbon monoxide in the atmosphere vary from 30-200 ppb CO (Khalil and Rasmussen, 1994), which is equal to 30-200 nmol/mol CO.

In this study, the ^{13}C and ^{18}O stable isotopes are examined. Isotopes are almost never expressed in absolute mole fractions, since these values are very small (order of 10^{-11}). They can be expressed in the isotopic ratio [R], generally, the ratio of heavy isotopes over the abundant isotopes, e.g. $^{13}R = \frac{^{13}\mathrm{C}}{^{12}\mathrm{C}}$ (order of 10^{-2}), a quantity useful for mass-balance calculations (Zeebe and Wolf-Gladrow, 2001). To improve precision, isotopic ratios are measured (and reported) relative to a reference gas, circumventing systematic errors. The measurement reports a deviation of the isotopic ratio of the sample relative to the isotopic ratio of a reference gas. This deviation, usually presented in per-mille (‰), is known as the δ value and is commonly used in isotope research. For example, $\delta_{\mathrm{SA,REF}}$ quantifies the deviation of the isotopic ratio in a sample (index SA) relative to a reference gas (index REF).

$$\delta_{\mathrm{SA,REF}} = \frac{R_{SA} - R_{REF}}{R_{REF}} = [\frac{R_{SA}}{R_{REF}} - 1] \cdot 1000‰ \tag{1}$$

A positive value means that the sample is enriched in heavy isotopes relative to the reference gas. A negative value indicates that the sample has less heavy isotopes, it is 'depleted' relative to the reference gas.

Since different laboratories use different reference gases, these values cannot be compared directly. To make this possible, the values are arithmetically calculated relative to an international standard. When the delta value of the sample versus the reference gas is known ($\delta_{\mathrm{SA,REF}}$) and the value of the reference gas versus the international standard is known ($\delta_{\mathrm{REF,IS}}$), then the δ value of the sample versus the international standard ($\delta_{\mathrm{SA,IS}}$) is given by equation 2.

$$\delta_{\mathrm{SA,IS}} = \delta_{\mathrm{SA,REF}} + \delta_{\mathrm{REF,IS}} + \delta_{\mathrm{SA,REF}} \cdot \delta_{\mathrm{REF,IS}} \tag{2}$$

All δ^{13}C and δ^{18}O values in this paper are reported versus Vienna PeeDeeBelemnite (V-PDB) and Vienna Standard Mean Ocean Water (V-SMOW).

2.2 Fundamentals of the stable isotopes

Stable isotopes do not decay and therefore their abundance in molecules is only affected by formation, removal and substitution processes (Farquhar, Graham D. Ehleringer and K.T., 1989; Conny, 1998). The δ^{13}C value of the bulk composition of plants with the C3 metabolic pathway for carbon fixation, ranges from -33 to -20‰ (Kohn, 2010). The composition of CO emitted by a source does not solely depend on the bulk composition, but also on the presence of fractionation, called the isotope effect: heavy and light isotopes reacts at different rates, causing a change in isotopic composition relative to the source (Zeebe and Wolf-Gladrow, 2001).

Isotopic fractionations arise due to e.g. chemical reactions, phase transition or diffusion processes, and generally, the underlying principle is mass dependent (Farquhar, Graham D. Ehleringer and K.T., 1989; Peterson and Fry, 1987; Stevens and Wagner, 1989; Zeebe and Wolf-Gladrow, 2001). These fractionations are called the kinetic isotope effect. However, since a reaction can occur in both directions, isotopic distributions are affected by both corresponding KIE's. When the interacting mixtures are in equilibrium, the final fractionation is determined by the sum of the KIE's (usually smaller than the individual KIE's), this is called the equilibrium isotope effect (Zeebe and Wolf-Gladrow, 2001).

Assuming that the photo-dissociation of molecules from plant material is an uni-directional process, and the only kinetic isotope effect occurring is due to a difference in vibrational energies, than the fractionation can be described according to the following principle. In a simplified manner, the vibrational energy of a diatomic atom can be represented as an one-dimensional harmonic oscillator, were two masses are attached by a spring. The vibrational frequency can be written as

(sources: Giancoli (2012); Criss (1999))

$$f = \frac{1}{2\pi}\sqrt{\frac{\kappa}{\mu}}, \tag{3}$$

where:

f	:	vibrational frequency	[s^{-1}]
κ	:	force constant	[Nm^{-1}]
μ	:	reduced mass	[m].

The reduced mass μ represents the effective inertial mass of two atoms (m_1 and m_2) in the molecule, and is written as

$$\mu = \frac{m_1 m_2}{m_1 + m_2}. \tag{4}$$

The vibrational energy is given by:

$$\mathrm{E_{vib}}=(\frac{1}{2}+\mathrm{n})\mathrm{h}f, \tag{5}$$

where:

h	:	Planck's constant	[Js]
n	:	quantum energy level	[0,1,2...].

Even at zero Kelvin, where $n = 0$, a molecule will still contain vibrational energy, this is called the zero point energy (ZPE) of a molecule (Johnson et al., 2002). When carbon monoxide $^{12}C^{16}O$ and $^{13}C^{16}O$ are taken as example, they possess a reduced mass of $\mu \simeq 12 \cdot 16/(12+16) = 6,9$ and $\mu \simeq 13 \cdot 16/(13+16) = 7,2$. The increased mass of the heavy isotope renders a lower vibrational energy, and this affects the zero point energy (ZPE), see equation 5. In summary, due to the higher mass, the ground state energy of the molecule is generally lowered, therefore more energy is needed for the molecule to dissociate, which results in a lower probability of the heavy isotope to dissociate (Zeebe and Wolf-Gladrow, 2001; Johnson et al., 2002). However, it should be noted that this is a simplified situation, since quantum mechanical tunneling is neglected (Alben et al., 1980).

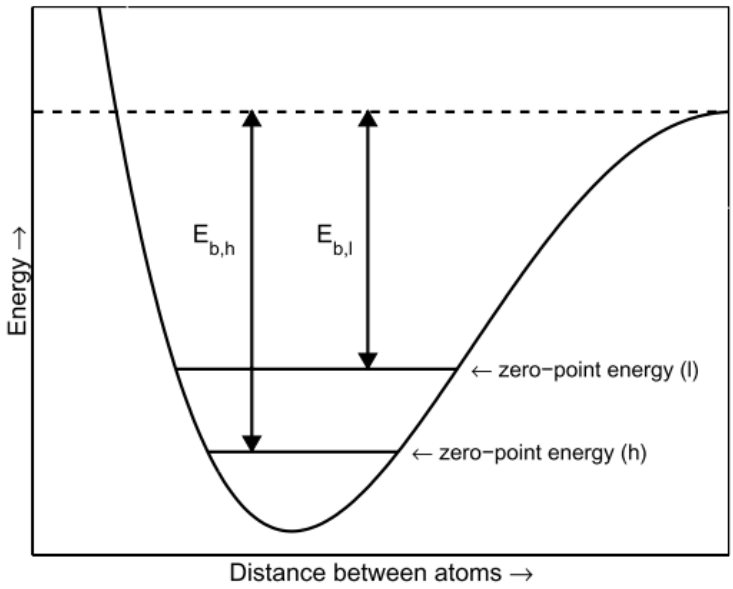

Figure 1: Schematic illustration of the binding energies of a diatomic molecule containing the heavy ($\mathrm{E_{b,h}}$) and the light ($\mathrm{E_{b,l}}$) isotopes, respectively. The zero point energy of the heavy isotope is lower, since the vibrational frequency is smaller, source: Zeebe and Wolf-Gladrow (2001).

2.3 Gas chromatography

A gas chromatograph (GC) is able to separate (multiple) constituent(s) from a gas. A GC is generally subdivided into three main components; the injector, a column and a detector. The injector injects the sample air, the sample air is referred to as the 'mobile phase'. The column, referred to as the 'stationary phase', separates the desired constituents and subsequently, the quantity of the desired constituent is measured by a detector (Ettre,1975). There are many and more different GC's types with there own specific injector, column and detector, depending on the desired application. The gas chromatograph used in this study is described in the material and method, section 3.2.

2.4 IRMS

Here, the physics of the IRMS is shortly discussed using CO_2 as example. First, the CO_2 is ionized, subsequently, it is accelerated due to a high voltage difference, and the beam of CO_2 ions is focussed using collimating slits and electronic lenses. The kinetic energy of the accelerated ion can be written as:

(source: Criss (1999))

$$qV = \frac{mv^2}{2} \tag{6}$$

where:

q	:	electric charge of the ion	[C]
V	:	voltage difference	[V]
m	:	mass of the ion	[m]
V	:	velocity of the ion	[m/s^2].

The charged ions are diverted due to a strong electric (or magnetic) field. Since the ionized isotopes possess different masses, their amount of diversion is different. The radius of the curvature can be calculated equating the electrostatic force, qE, with the centripetal force, $mv^2/2$:

$$r = \frac{mv^2}{qE} \tag{7}$$

where:

r	:	radius of the curvature	[C]
E	:	electric field	[N/C]

Since each isotope is has its own radius of curvature, the beams are separated. Subsequently, collectors are positioned in the trajectory of the beams. The abundance of the isotopes is counted by the collectors and the ratios are calibrated against a reference gas with known isotopic ratio and mole fraction. Henceforth, the isotopic composition and molar fraction of the sample are determined.

3 Materials and methods

3.1 Plant material

The investigated plant is a Caryota Mitis (commonly known as fishtail palm), a genus of the palm tree and using the C3 metabolic carbon fixation pathway. This plant was located in our coffee room, and was not exposed to direct sunlight. It was watered every week and the room temperature remained relatively constant across all tests (estimated to be 21 $\pm$ 2°C). This site and plant offered convenient characteristics: the plant was easily accessible, a smooth stem for easy sealing, and the plant was not exposed to UV-radiation. Moreover the outdoor trees did not have any leaves at the start of this research.

3.2 Gas chromatograph

The gas chromatograph used in this study (the Peak Performer 1, model 910-105) includes a chromatographic column (molecular sieve) and a mercury UV detector. The molecular sieve separates the CO (and H_2) from the air bulk. The CO released from the column passes over a mercury oxide (HgO) bed, and reduces the HgO, a proces that releases Hg vapor. The Hg vapor will block radiation between a UV-source and a photo-detector, thereby influencing the signal generated by the photo-detector. The UV detector signal is therefore proportional to the carbon monoxide in the air sample, subsequently, a software program calculates the corresponding CO concentration.

3.3 GC-IRMS system

The analytical setup used in this study uses the conceptual technique developed by Stevens et al. (1972). This technique does not measure the CO directly, but converts it to CO_2. Extracting CO directly from air is problematic due to low abundance and the boiling point of CO being close to that of air, making thermally based traps cumbersome. Molecular sieve based techniques can induces biases at low concentration when high precision is required (Brenninkmeijer et al., 1999). High precision mass spectrometry is often specially developed to measure CO_2, therefore, Stevens et al. (1972) developed a method which first removes all

the CO_2 from the sample air, followed by the oxidation of CO to CO_2, subsequent trapping of the CO_2 and thereafter the CO_2 is supplied to an IRMS.

In the GC-IRMS setup, described by Pathirana et al. (2015), the sample air is transported through the system by a carrier gas of ultra-high purity helium, a schematic illustration is given in figure 2. The CO_2 and H_2O of the sample are absorbed by a chemical trap. In the chemical trap, the sample air is first exposed to ascarite, which converts CO_2 to H_2O, and thereafter to magnesium perchlorate, which absorbs the H_2O. In the first cryogenic trap, the CO_2 is condensed using liquid nitrogen, while other gases are removed by a vacuum pump. It is important to exclude all the N_2O, since N_2O has the same mass as CO_2. The CO is oxidized to CO_2 using the Schutze Reagent (Smiley, 1949). In the second and third cryogenic trap, referred to as pre-concentration and focus trap, respectively, the CO_2 is trapped in a smaller volume, increasing its concentration. The gas chromatograph further purifies the CO_2 from other trace gases left in the sample. Subsequently, the elutant is transported into the IRMS (Finnigan Deltaplus XP), which accurately counts the relative quantity of ion masses (m= 44, 45 and 46). The system is able to measure the mole fraction and the δ values (both $\delta^{13}C$ and $\delta^{18}O$) with a precision of 0,5 ppb and 0,1 ‰, respectively. Each sample is measured two times; for one measurement the system uses 150 mL of sample air with a minimal sample pressure of 1,4 bar. To make two measurements from the same sample possible, the glass flask is filled with sample air until a pressure of 1,8 bar is reached.

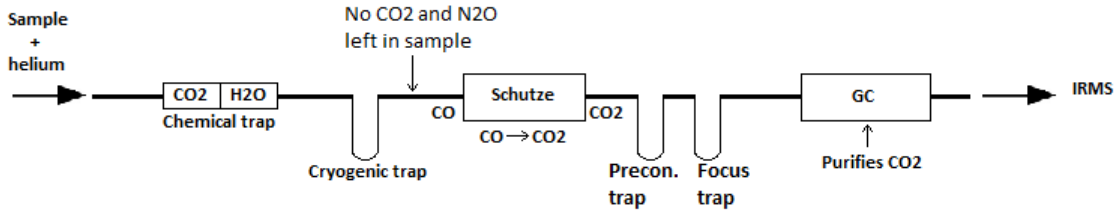

Figure 2: Simplified schematic illustration of the GC IRMS system at the IMAU laboratory. With the chemical trap comprising of ascarite and magnesium perchlorate. Precon. is short for the cryogenic pre-concentration trap.

3.4 Method

3.4.1 Sampling

To determine the isotopic composition of CO emitted by the plant, the CO is emitted in a contained amount of air. The added carbon monoxide induces an isotopic change in the

contained amount of air. To achieve this situation, the branch was sealed air tight with a plastic bag, containing approximately 5-7 liters of dry atmospheric air. Samples were taken by sucking out air, with a custom made pump system. The air from the bag was led through a drying trap (magnesium perchlorate) and particulate filter of 7 micron, into a battery powered pump (KNF, type pm 2287-86), through a barometer, into a 1 liter volume glass flask (Normag, Ilmenau, Germany), see figure 3. The glass flasks were pre-evacuated before being used for sampling. The samples were filled up to 1,9 bar, the pressure was monitored by placing a pressure gauge in serie. A sample was obtained right after the branch was sealed (t_0), samples taken in succession each bridged a certain time interval. A change in isotopic composition occurred during the time interval, corresponding to the increase in mole fraction. Knowing these two values, the isotopic composition of the source can be calculated, as will be explained hereafter (section 3.5).

Tests were performed under different situations (*living branch, stressed branch* and *cut off / senescent branch*), described in table 1. Three branches of the same plant were tested, referred to as, branch 1, 2 and 3. This research did not have the scope to investigate the dependence of the isotopic signature on light intensity/wavelengths or the absolute emission, therefore, light intensity is not measured. To investigate if there is a different mechanism for thermal and photo-degradation, samples were taken in presence and absence of room (UV excluded) light radiation. The cut off branch is used for these tests, senescent leaves generally have higher emissions (see introduction), which increases the reliability of the calculations. All isotope samples are obtained by the following procedure:

1. First, the bag is sealed around the branch.

   The bag is cut open, providing enough space to enclose the branch. A small tunnel is welded surrounding the stem, using an 'Audio Elektra, type 381 ps' welding device, which consists of a 30cm long straight clamp of approx. 5 mm wide, it can melt two layers of plastic together by heating the clamp for a short period of time. The bag is now welded air tight and the tunnel created encompassing the stem is tightly wrapped with simple tape.
2. The bag is 'flushed' and afterwards filled with 5 to 7 liters of dry atmospheric air.

   This 'flushing' done by filling the bag with dry atmospheric air, and subsequently sucking out almost all air (less then ∼0,2 L left) with a vacuum pump (KNF, type mpu 2134 n920-208). This is repeated twice to remove almost all air after the welding, suppressing unknown adverse affects caused by the welding (thus heating) of the plastic.
3. The first flask is filled with sample air.
4. Next samples are taken after a certain time interval, generally 3 samples are taken. After the last sample is taken, the bag is removed.

**In the beginning, the air was removed by pressuring the bag lightly by hand (test 1-7, of 19 total). Not all air could be extracted using this technique, henceforth the vacuum pump was used, able to suck out almost all air.*

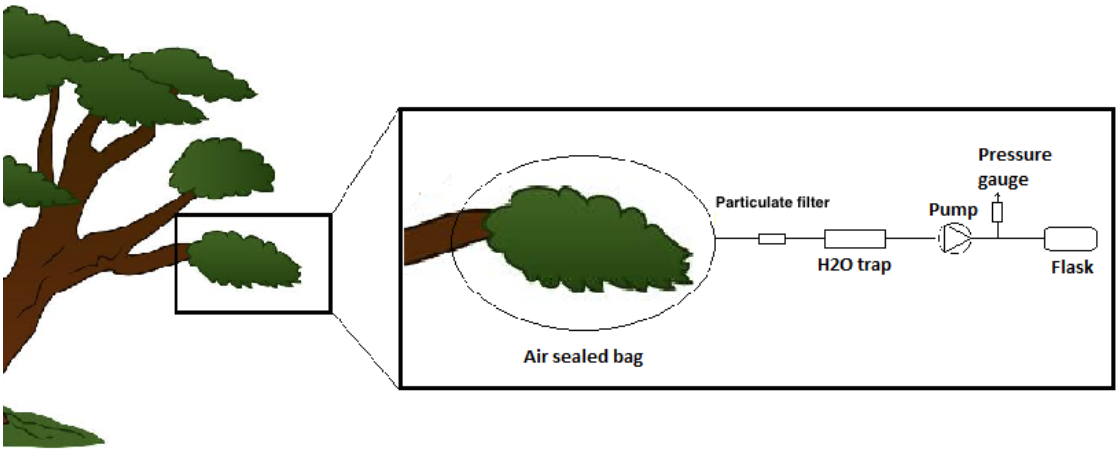

Figure 3: Schematic illustration of the sampling method. A minimum of two glass flasks were filled with air. The first sample is taken at the beginning, to capture the initial mole fraction and isotopic composition, and the second sample is taken after a certain time interval. In most tests, multiple samples are taken, satisfying that, the time interval between samples is long enough to induce a measurable change in isotopic composition.

Table 1: Types of experiments.

Type	Method	Additional information	Time interval	n
Living branch	#1	Branch was enclosed in normal conditions (in tact), two different branches were tested.	1 to 1.5 hrs	5
Stressed branch	#1	The leaves were stressed lightly, first, a total of 4 folds were made in the leaves and secondly another 4 folds were added. This was done while branch was already sealed in the bag, branch 2 was tested	1 hr	1
	#2	The branch was stressed more severely by folding and squeezing the leaves as much as possible, while the branch was already sealed in te bag, branch 2 was tested.	1.5 hrs	1
	#3	The leaves were damage with scissor, making more cut-through cuts. This was done just before the bag was sealed, 'branch 3' was tested.	1.5 hrs	1
Cut off / senescent branch		Samples were taken right after the cut (day 0), and after 1, 4, 5, 8, 12 and 15 days. The bag was still sealed around the stem to exclude affects of plant liquids escaping (and evaporating) easily through the stem veins.		7
	#1	'Normal' test, branch was exposed to room light, day 0 and 4.	1.5 hrs	2
	#2	Firstly, the branch was exposed to room light and secondly, the branch was kept in dark by enclosing it with non-transparent garbage bags, day 1, 5, 8, 12 and 15.	1.5 to 4 hrs	5

3.4.2 Sampling bag stability tests

At the beginning of the investigation, the type of sampling bag (plastic) that was going to be used had to be determined. The plastic had to satisfy the following characteristics: transparent, flexible, to avoid adverse pressure effects, and CO inert, thus not affecting the carbon monoxide mole fraction. Almost all (or all?) plastics are subjective to photo-degradation, thereby likely to emit CO. The plastic bags had to be tested whether they emit CO in quantities that could interfere with the experiments. The CO inertness was tested using the Peak Performer 1, which is capable of measuring the mole fraction of carbon monoxide and hydrogen with a typical precision of 1 ppb.

UV transparency tests were performed with a Waldmann UV meter 585-100, comparing the quantity UV-radiation [Wm^{-2}] with and without obstruction of the plastic material.

Three different types of bags were tested: FEP, SKC 46336, SKC 50869, the chemical materials of the latter two bags are patented by the SKC Ltd. company. One bag was custom made from a sheet of Fluorinated Ethylene Propylene (FEP). The plastic was folded into an appropriate size and 'welded' together with the previously mentioned welding device (Audio Elektra, type 381 ps). For these tests, all bags were air tight, having one single pass through, connected to a valve. The tests were conducted by the following 6 step procedure.

1. The bags were filled with approximately the same amount of air (the order of magnitude, expected to match actual experiment).
2. The Peak Performer 1 (PP1) measured a reference gas.
3. The bags were connected to the PP1. One single test of 5 measurements were taken to allow the PP1 to equilibrate, which would take around 30 minutes. To prevent photo-degradation to occur during the tests, the bags were covered with blankets.
4. They were exposed to room light for 1 to 5 hours.
5. The bags were remeasured with the PP1.
6. The reference gas was measured to check whether the PP1 was stable.

3.4.3 Blank measurements

Emission tests
The sampling bag stability tests were only a single experiment result (n=1) in laboratory room light, more blank tests were performed with the PP1 simultaneous to each 'isotope experiment'. The same procedure was followed as explained in the previous section 3.4.2, generally, 2 or 3 blanks were exposed to room light during the identical time interval of the corresponding isotope experiment. This resulted in a situation were the blank was exposed to the same room light for the same amount of time as the isotope sampling bag, enabling the possibility for correction.

Isotope tests
Moreover, both emission and the CO isotopic signature of multiple 'FEP bags' were measured with the GC-IRMS. This was done to allow a correction for CO emitted by the bag instead of the plant. Multiple bags (7) were created during the course of this research period, because they had to be cut loose from the branch after each experiment, making them smaller. The same bags used for the plant-isotope tests, were used for this experiment.

The empty bags were were placed on the ground and generally similarly sampled as the plant isotope-tests, as described in section 3.4.1, although the procedures (flushing and sampling) were conducted in the laboratory. During these procedures the bag was kept in darkness for no more then 40 minutes, causing negligible CO emission (as proven later on in the result section 4.1, figure 6). Meaning, the emission of the bag started when exposed in the same experiment site, the coffee room.

To test if there was an influence of the welding, one bag was welded before it was flushed, identical to the plant-isotope tests. Another bag was placed in the shadow to investigate if the isotopic composition of the emitted CO is influenced by the amount of light.

3.4.4 Preparing plant material for bulk analysis

For the bulk analysis, which rendered the carbon isotopic composition of the leaf, the plant material had to be grinded to a powdered substance. In the first attempt, a leave (of branch 1) was kept in the oven for two days at 80 °C, subsequently, the dried leaf material was placed in a conventional coffee miller. It turned out, that the nerves of the leaves were not easily powdered and kept their stem-structure. The second attempt, a porcelain mortar, pestle and liquid nitrogen were used. Liquid nitrogen was sequentially added in the bowl to freeze the plant material and make in more susceptible to crumble. Some water had condensed on the powder during the process. Subsequently the powder was placed in the oven for a few hours and afterwards, the powder was sent to the stable isotope facility of the integrated laboratory at the Utrecht University.

3.5 Calculating the CO isotopic composition

To calculate the isotopic composition of the plant-emitted CO, the 'Keeling plot' analysis can be used, as discussed by D. Pataki (2003). A calculation of the $\delta^{13}C_{source}$ will be shown as example. By sealing the branch air tight with a bag, the air is contained, and the following formula can be written for the mole fractions (equation 8),

$$x_f = x_i + x_s \tag{8}$$

where,

x_f	:	final mole fraction	[ppb CO]
x_i	:	initial mole fraction	[ppb CO]
x_s	:	added mole fraction by the source	[ppb CO].

The isotopic composition of the CO which was added to the initial air in the bag can be calculated using equation 9,

$$\delta^{13}C_f \cdot x_f = \delta^{13}C_i \cdot x_i + \delta^{13}C_s \cdot x_s \tag{9}$$

where,

$\delta^{13}C_f$	:	final δ^{13}C value	[‰]
$\delta^{13}C_i$	:	initial δ^{13}C value	[‰]
$\delta^{13}C_s$	:	δ^{13}C value of the source	[‰]

By substituting x_s from eq. 8 into eq. 9, a formula can be written in the format of $y = a \cdot x + b$, with the inverse of x_f for x and $\delta^{13}C_s$ for b.

$$\delta^{13}C_f = (\delta^{13}C_i - \delta^{13}C_s) \cdot x_i \cdot \frac{1}{x_f} + \delta^{13}C_s \tag{10}$$

When the added CO would be assumed infinite ($x_s \longrightarrow \inf$), thus $x_f = x_s$, the limit would render the δ value of the source. The delta value of the source can be obtained graphically: when fitting a straight line to the time evolution of $\delta^{13}C_f$ versus $1/x_f$, the source signature ($\delta^{13}C_s$)) is given by the y-intercept (see figure 4), this is the so-called "Keeling plot" analysis. A larger relative increase in mole fraction, increases the reliability of the calculation.

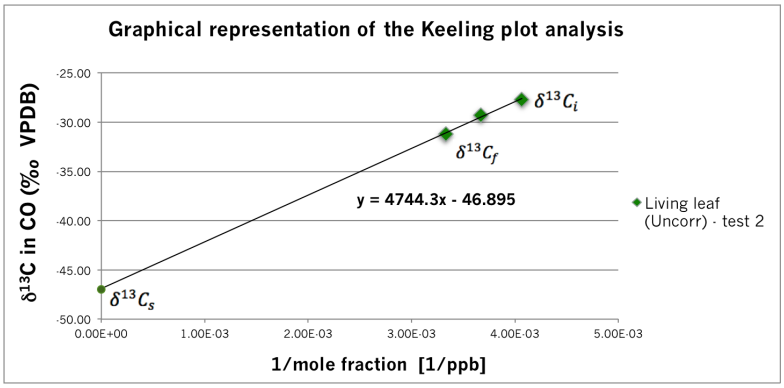

Figure 4: Graphical representation of the keeling plot method given as equation 8. Three samples are collected and measured, the first samples containing the initial value ($\delta^{13}\mathrm{C_i}$), and subsequent samples ($\delta^{13}\mathrm{C_f}$) are mixed with the more depleted plant-emitted CO ($\delta^{13}\mathrm{C_s}$).

During the progress of this study, it was found that the bags were emitting CO and therefore, the previously calculated increase in mole fraction and change in isotopic composition was a induced by two sources. Consequently, a correction had to be made for the bag-emitted CO, the correction is implementing using the following formula's. Since the increase in molar fraction is now including the bag emission, it can be written as:

$$\Delta x_{tot} = \Delta x_{bag} + (\Delta x_{tot} - \Delta x_{bag}) \tag{11}$$

where,

Δx_{tot}	:	total increase CO	[ppb CO]
Δx_{bag}	:	total increase CO of the bag, based on averaged blank emission.	[ppb CO]

Hereby, $\Delta x_{tot} - \Delta x_{bag}$ represents the plant-emitted CO. The following equation renders the corrected value for δ^{13}C or δ^{18}O, if either the δ^{13}C or δ^{18}O is filled in for the δ symbols,

$$\delta_{\mathrm{corr}} = \frac{\delta_s \cdot \Delta x_{tot} - \delta_b \cdot \Delta x_{bag}}{\Delta x_{tot} - \Delta x_{bag}} \tag{12}$$

where,

δ_{corr}	:	corrected delta value	[‰]
δ_s	:	the uncorrected delta value, as calculated by equation 10.	[ppb CO]
δ_b	:	CO signature of the bag, based on the averaged blank signature	[‰].

The final errors presented are calculated, using statistical quadratic error propagations. For example, if variables x and y are multiplied or divided in function $f(x, y)$, they are

treated as shown in equation 13. If these variables are added or subtracted, they are treated as shown in equation 14. Standard deviations are presented for averaged values using the excel function 'STDEV', the range encompassing 68% of the values.

$$\frac{\sigma_f}{f} = \sqrt{\frac{{\sigma_y}^2}{y} + \frac{{\sigma_x}^2}{x}} \tag{13}$$

$$\sigma_{\mathrm{f}} = \sqrt{{\sigma_y}^2 + {\sigma_x}^2} \tag{14}$$

4 Results

4.1 Bag tests

The emission of the three different bags exposed to laboratory room light are shown in figure 5. The bag with the lowest emission rate, was tested for UV-transparency and CO emission under UV-radiation. A transparency of $\sim 90\%$ was measured with a Waldmann UV-meter 585-100 (data not shown). The CO emission of the bag under UV-radiation is shown in figure 6.

As can be seen in figure 5 and 6, the FEP material emitted the least CO per hour. The original plan was to eventually perform tests outdoor, being more representative for 'real-world' plant emission. However, UV-radiation increased the emission of the bags substantially, therefore, it was decided to continue with the Caryota Mitis and test different situation (stressed and cut off). These situations were also more likely to emit more CO, which reduces the relative impact of interference.

After analysing the blank bag emissions, the flux showed to be high enough to interfere with low plant-emission isotope experiments. Blank emissions sometimes varied substantially, making correction with the corresponding blanks per isotope test (n$\leq$3) unrepresentative, see appendix B. Therefore, all blank tests were averaged (n=39), leading to an emission of $6,5 \pm 3,1$ ppb CO/hr.

The isotopic composition of the blank-emitted CO were sampled using the method as described in section sampling 3.4.2. No notable deviation is observed for the 'freshly welded' bag 6. Bag 4 (placed in shadows) emitted little CO, inducing an isotopic change close to the precision of the GC-IRMS, making this calculation unreliable and it is therefore discarded. In continuation of this research, an average (bag 4 omitted) is taken from these datapoints to correct for the plastic-emitted CO, see table 2. The correction is implemented according to the formula's given at the calculation section 3.5. The spread in δ^{13}C is quite substantial (ranging from $-82,6 \pm 3,2$ to $-60,4 \pm 1,6$‰), causing high errors when the correction is implemented. The δ^{18}O values were more consistent, ranging from $8,9 \pm 1,2$ to

$13,4 \pm 1,0‰$. The errors, of the emission and δ values, are propagated using the statistical method described in section 3.5 and are henceforth used in the graphs.

Table 2: Averaged CO stable isotope values of ^{13}C and ^{18}O emitted by FEP (from 'bag 2, bag 3-2, bag 6 and bag 3-1').

Average $\delta^{13}C$	Standard deviation	Average $\delta^{18}O$	Standard deviation
-73	11	11	2

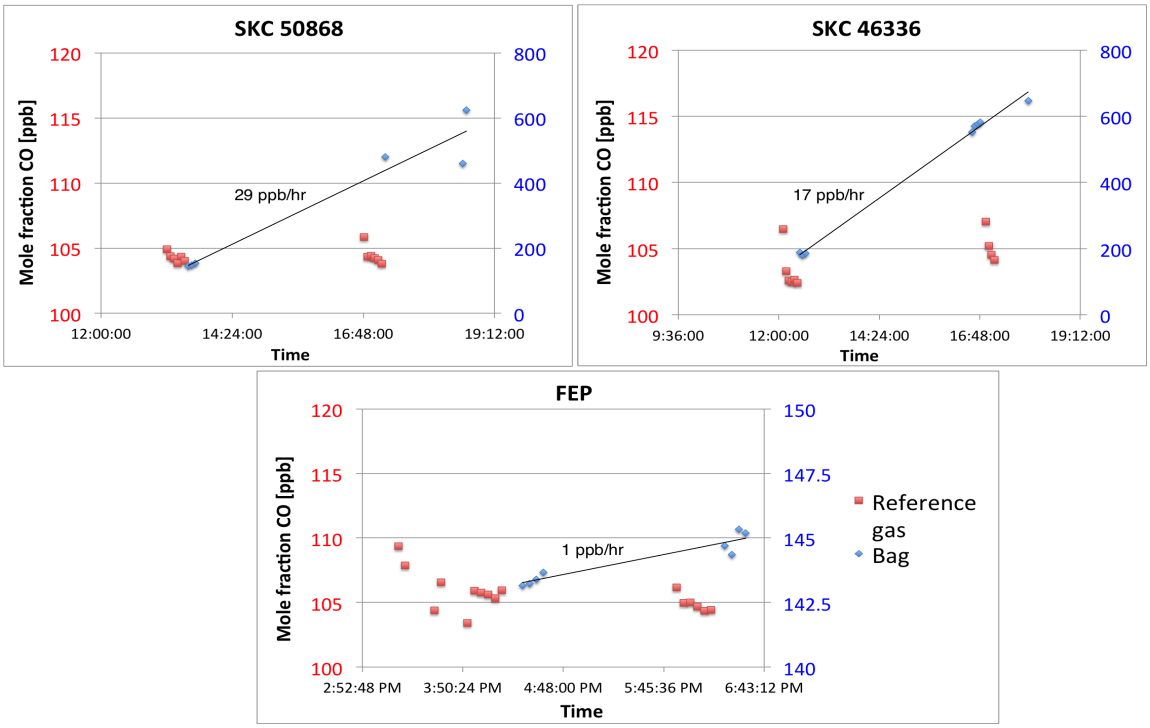

Figure 5: The CO emission of the three types of bags in laboratory room light as function of time.

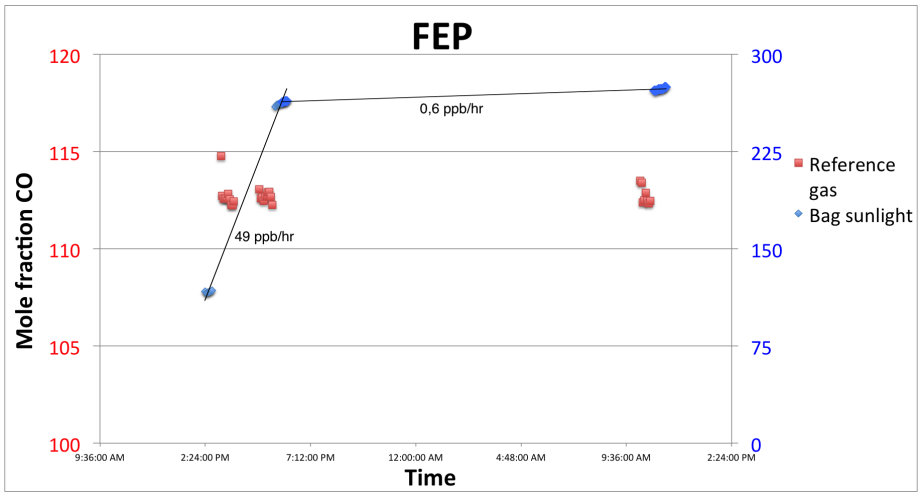

Figure 6: Three data series were measured, spanning two time intervals. In the first time interval the bag was exposed to sunlight for approximately 3 hours, during the second time interval, all radiation was blocked (darkness).

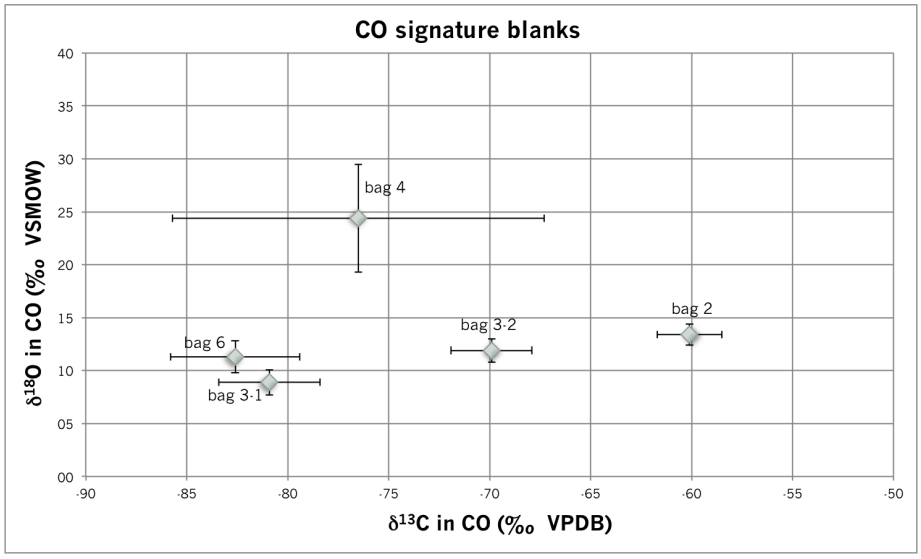

Figure 7: The bag-emitted CO signatures, the bags were exposed in the same coffee room, filled with the same (amount of) air as used for the isotope sampling tests. Bag 6 was welded and flushed before sampling, and bag 4 was placed in the shadows. Datapoint 3-1 and 3-2 correspond to the same bag, sampled on different days.

4.2 Living branch

As shown in section 4.1, all samples should be corrected for the CO emitted by the sampling bag. In some tests, the emission of the living leaf was observed to be lower or near equal to the averaged emission of the bags (see Appendix C), therefore, the change in isotopic composition was expected to be greatly influenced by the bag-emitted CO. Likewise, a small over- or underestimation of the emission or delta value, will induce a big impact on the corrected value. It should be noted that implementing the correction did make the results more coherent as would be expected, see Appendix A and the discussion section.

Since the propagated uncertainty of the bag-δ^{13}C values was large (see table 2), the corrected δ^{13}C values were most prone to high imprecision. Therefore, the corrected δ^{13}C values are used to evaluate if a corrected test should be considered reliable, see figure 8A. Based on the previously mentioned arguments and evaluation of figure 8A, it is decided that tests with a plant/blank emission < 2 are discarded.

The signatures emitted by living leaf, passing this reliability test, are shown in figure 8B, the average plant-emitted CO of these tests was $20,7 \pm 0,5$ ppb/hr. Two different branches (branch 1 and branch 2) were tested, yet only tests with branch 1 (with a larger foliage area than branch 2) emitted enough CO to be considered reliable. Still, the calculated δ^{13}C values had high errors, moreover, the values varied quite widely, ranging from $-43,1 \pm 13,7$ to $-29,6 \pm 12,2$‰. The δ^{18}O was less subjected to high errors, the values ranged from $37,9 \pm 4,6$ to $42,3 \pm 7,3$‰.

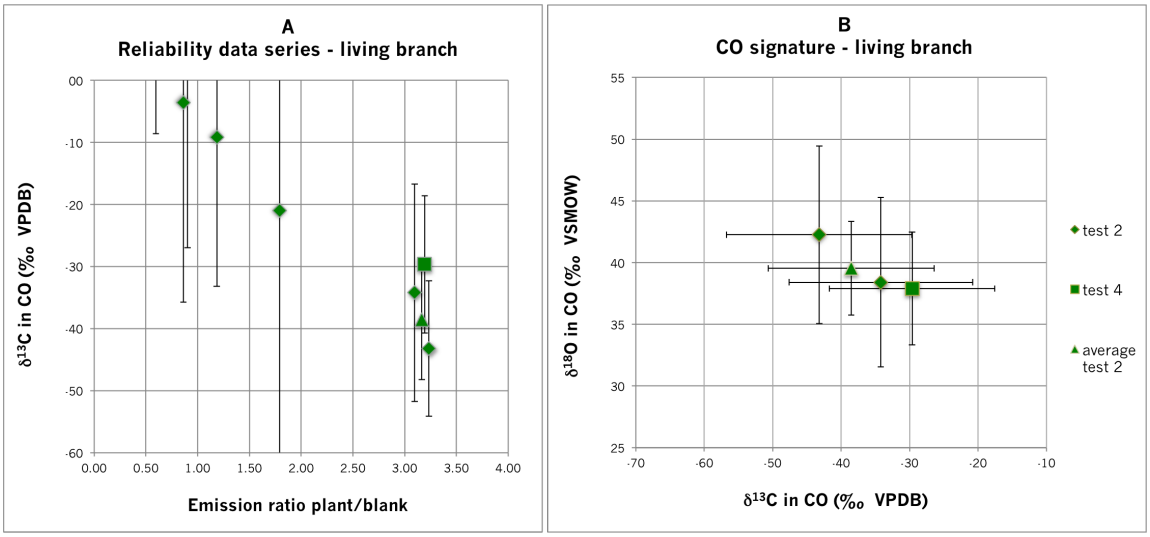

Figure 8: A: The δ^{13}C values versus the emission ratio plant/blank are shown. This graph points out that correcting the δ^{13}C value when low plant emissions are observed, leads to very poor accuracy and reliability. B: The CO signatures of 'living branch' tests emitting enough CO to be considered reliable.

4.3 Stressed branch

Evaluating figure 9A, data-points with a plant/blank ratio below 3 are discarded to avoid large errors. As described in table 1, these branches were not stressed in the same manner. In short, method #1 was 'gently' stressed, up to method #3, which was severely stressed. This is evidenced by the increasing rate of plant emission calculated, $23, 57$ and $265 \pm 0, 7$ ppb CO/hr, respectively to the ascending order of intensity stressed (see appendix A).

In figure 9B it can be seen that the δ^{13}C values of the different tests varied from $-42, 2 \pm 4, 6$ to $-30, 7 \pm 12, 5$‰. The δ^{18}O values varied very much, from $6, 2 \pm 1, 2$ to $32, 3 \pm 6, 9$‰.

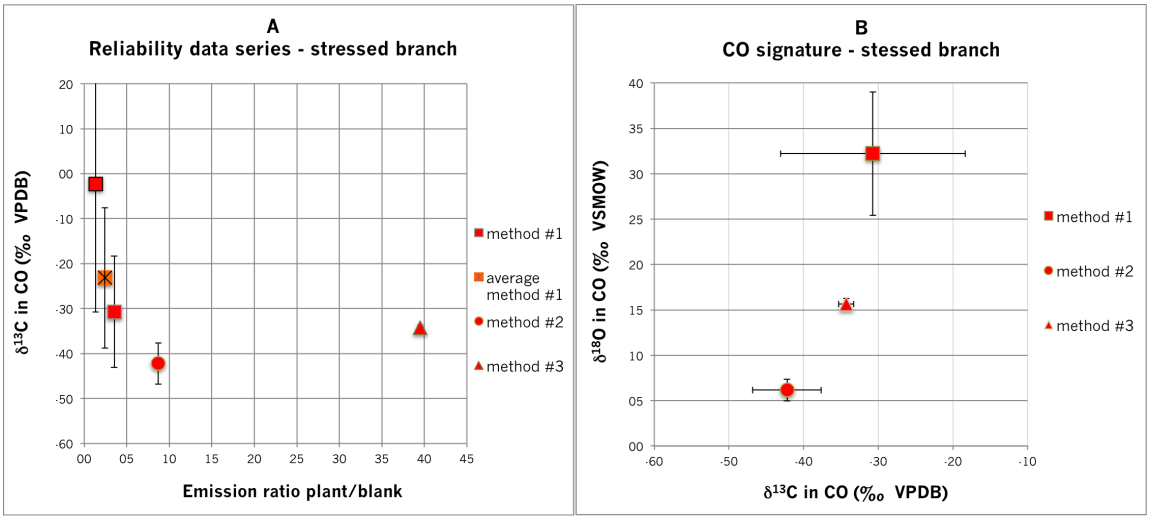

Figure 9: In graph A, the δ^{13}C values versus the ratio plant/blank emission are shown. Graph B shows the CO signature while the branch was stressed, Method #1 being least stressed, method #2 moderately and method #3 was stressed severely.

4.4 Cut off / senescent branch

Samples are taken under normal room light and in dark conditions, as described in table 1.

Due to the higher emission of the cut off branch, the precision of the δ values increased substantially, with the averaged emission in light being 71 ± 43 ppb CO/hr. The emission of the cut off branch was expected to increase as it became older, however, this was not observed, see figure 11. The ratio of dark/light emission did increase linearly from $43 \pm 0,7$ on day 5 to $87 \pm 0,7\%$ on day 15 (figure 11).

In figure 10, the relatively high inaccuracy and very high ^{18}O enrichment of datapoint day 5 in dark, is eye-catching. For this test, the two GC-IRMS measurements of the third sample reported moderately deviating values. Subsequently, it was measured a third time, reporting in the middle of the two values. This abnormal value should be considered less reliable. The δ^{13}C values vary in a similar range compared to the previous tests, $-29,5 \pm 1,6$ to $-47,5 \pm 1,3$‰. Similar to the stressed situation, the δ^{18}O varied a lot, and even dropped to depleted values, ranging from $-7,8 \pm 1,1$ to $27,7 \pm 1,7$‰ (datapoint 5 in dark omitted).

To present these results in more detail, plots as function of days are presented in figure 12. When comparing the dark (solely thermal degradation) and light (thermal + photo degradation), and without considering data-point day 5, the thermal emitted CO δ^{18}O values are almost identical to the light δ^{18}O CO values. While the δ^{13}C values in dark

(thermal degradation), are consistently less depleted relative to the photo- and thermal degradation (figure 12).

Extra values discarded:
Although the GC-IRMS seemed to be reporting correct (considering minimal deviation between both flask-measurements, and the multiple corresponding reference values), three results were found to be conspicuous. First, the interval exposed to room light of test day 0 and the interval in dark of test day 1, both showed a minor uptake of CO, which at these concentration was never observed before by plant material. Secondly, the second time interval of test day 4, which was exposed to room light, showed an increase of 7 ppb/hr, while the previous interval, also exposed to room light, showed an emission rate of 50 ppb/hr. The reason for these strange results was difficult to explain and remained unknown, henceforth they are discarded, all results (including all discarded) can be found in Appendix C.

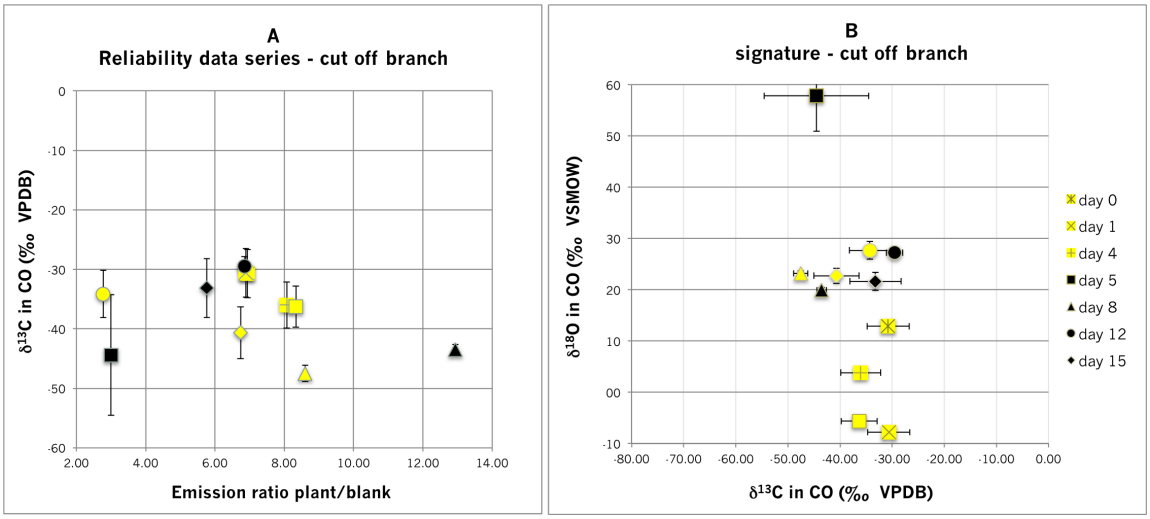

Figure 10: in graph A, the δ^{13}C values versus the ratio plant/blank emission are shown, tests with ratio's < 3 (the first two data-points) are discarded because of the unreliability. In graph B, the CO signatures corresponding to the days after the cut are presented.

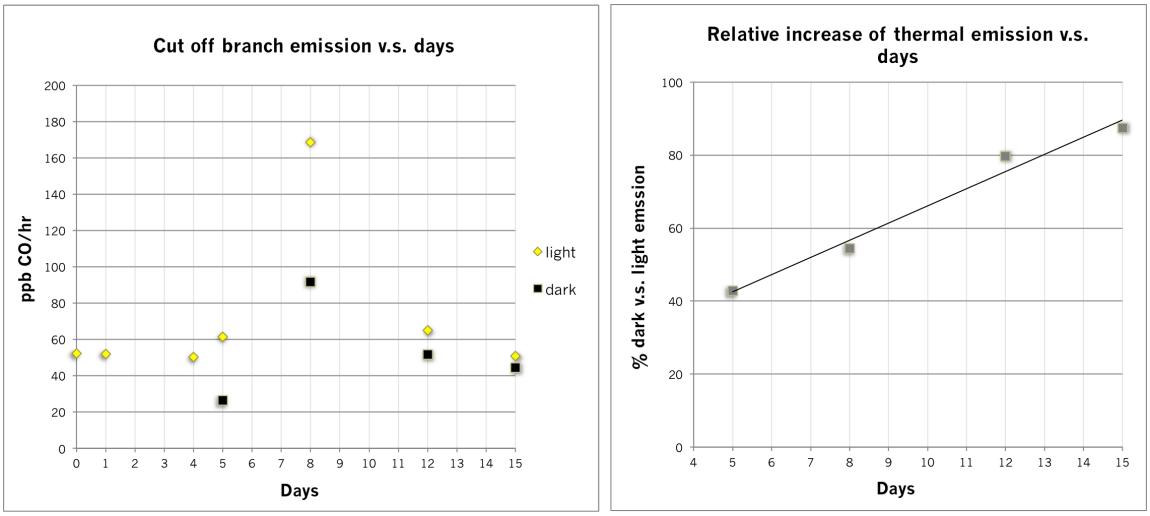

Figure 11: The emission of CO (in mole fraction) as function of days, with an exceptional high emission on day 8. The absolute emission is not clearly increasing as function of days (left graph), however, the share of emission being caused by thermal degradation is indicating to increase (right graph).

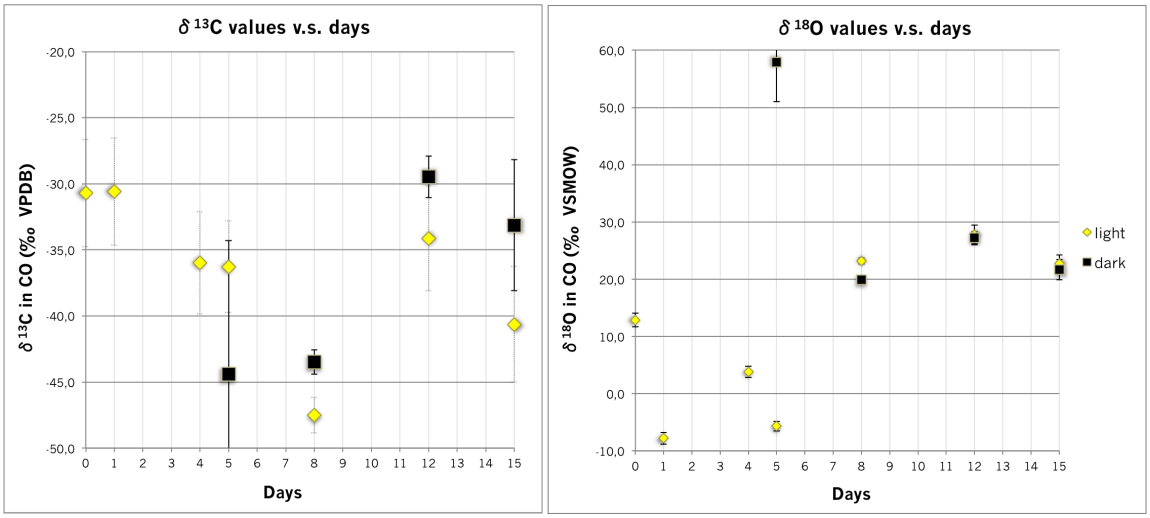

Figure 12: The δ^{13}C and δ^{18}O values as function days.

4.5 Overview results

The signature and SD's averaged over all data-points are shown in table 3. It should also be noted that, considering the large variations, a small number of tests were conducted (and considered reliable), thus the averaged values and SD's should be treated accordingly.

Comparing the averaged δ^{13}C values of the different situations, they match quite well. However, the individual δ^{13}C values showed to vary and some δ^{13}C values possessed large standard deviations, which were propagated into the averaged value.

The individual δ^{18}O values possessed higher precisions compared to the δ^{13}C values. The large standard deviations of the stressed- and cut off branch exposed to light were dominantly caused by significantly varying δ^{18}O values, and not by errors.

Living leaf tests showed to emit significantly more ^{18}O enriched δ-values. It is also interesting to see that the CO emitted in dark (solely thermal) was more enriched in both ^{13}C and especially ^{18}O. Moreover, it can be noted that the averaged δ^{18}O value of the cut off branch in light is actually close to the two more severely stressed branches, being $6,2 \pm 1,2$ and $15,7 \pm 0,6$‰. The external laboratory who performed the analysis of the bulk plant material reported a δ value of $-34,1 \pm 0,25$‰.

*For the calculation of the averaged cut-off - thermal, test day 5 in dark is left out due to the unreliability and large inconsistency.

Table 3: Averaged δ^{13}C and δ^{18}O values of carbon monoxide.

	Average δ^{13}C	SD	Average δ^{18}O	SD
Living branch	-36,3	5,8	39,6	2,0
Stressed branch	-35,7	5,9	18,0	13,2
Cut off - thermal + photo	-36,5	6,0	11,0	14,4
Cut off - thermal	-35,4	7,3	22,9	3,8
Average all	-35,6	5,7	23,1	17,2
Bulk carbon composition	-34,1±0, 25			

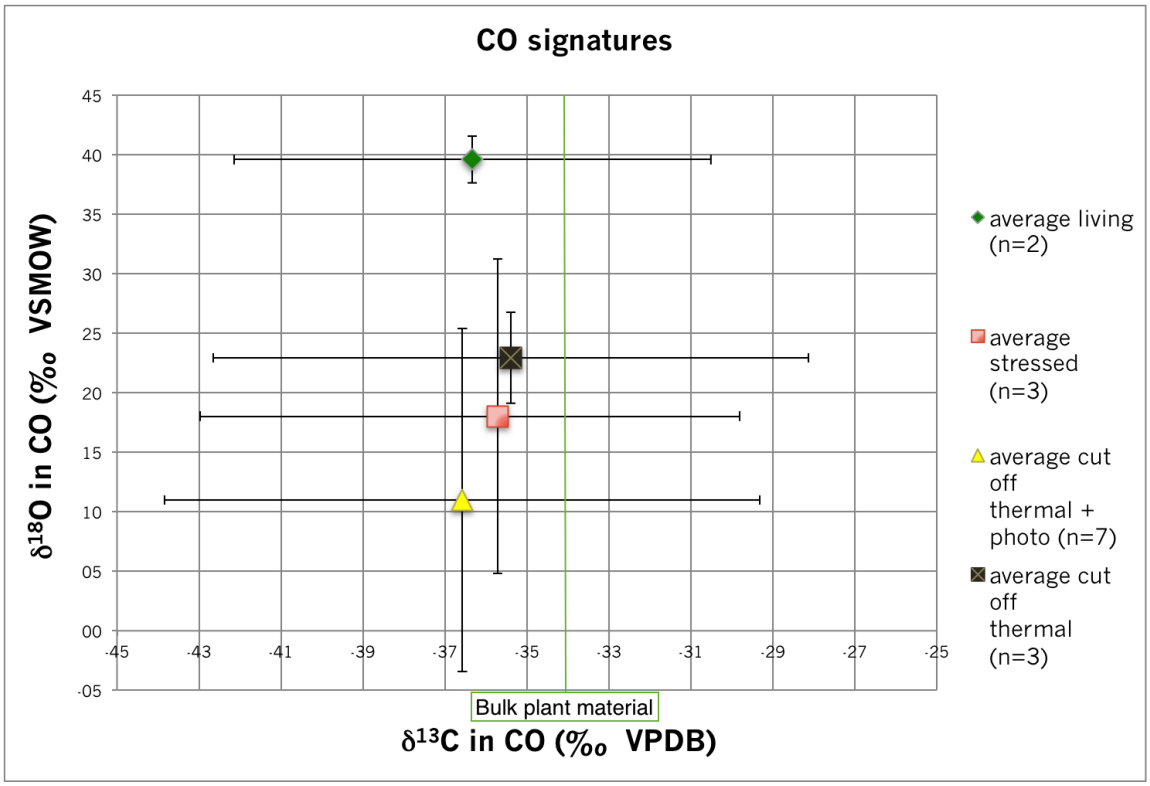

Figure 13: The averaged plant-emitted CO δ values under different situations (*living branch, stressed branch* and *cut off / senescent branch*) are presented in the same CO signature space. The green line is representing the δ^{13}C value of all carbon based constituents of the plant material.

5 Discussion, conclusions and outlook

CO emission from the bags proved to be a bottleneck for some experiments after correction (especially for 'living branch' tests), however, despite the high inaccuracy as result of the blank signature, one would expect values to become more coherent after correcting them. Surprisingly, the uncorrected values were more coherent than the corrected ones, this was true for all tests, see appendix A for uncorrected δ^{13}C next to the corrected values. This would suggest that the correction is wrong (overestimated), yet, the measured average emission (n=39) and corresponding isotopic composition (n=4) cannot be neglected. Bidwell and Fraser (1972) did measure an uptake of CO by leaves, possibly, the CO released by the bag and plant, was absorbed and emitted simultaneously, with a net emission. The bag-emitted CO signature would be lost after being absorbed and subsequently emitted by the

plant. However, in Bidwell and Fraser's experiment, the leaves were exposed to unnatural high concentration of CO (mostly $\sim$ 1ppm CO, $\sim$ 5 times higher compared to our experiments), and still the uptakes were low (see report for more detail). Moreover, the precision of the instruments in those years is doubtful (no errors are reported) and they made a rough estimation that the uptake would be linearly proportional to the concentration, which can not be proven with their results.

The spread of all the δ^{13}C values was large, but quite consistent, all δ^{13}C values calculated, fell within $-47,5$ and $-29,5$‰. Therefore, the averaged values of the different situation, matched quite well. Moreover, since these high variation were observed in all measurements, no conclusions can be made from the observed δ^{13}C cut off values versus days.

The δ^{18}O values of CO emitted by the living branch were observed to be significantly higher compared to the stressed and cut off tests, although only 2 tests, with 3 datapoint were taken into account.

The δ^{18}O values of the stressed leaf tests varied from 6,2 to 32,3‰, suggesting that the origin or the reaction mechanism of the oxygen atom changed. Possibly, this could be appointed to the fact that (more) carbon atoms interact with oxygen (containing a different isotopic composition) released when the plant was stressed, perhaps involving oxygen from plant liquids. During method #1 almost no plant fluids appeared, method #2 showed some liquids and during method #3 leaves were cut-through with a scissor multiple times, leading to a lot of plant liquids. However, one would expect a correlation between the amount of fluids and the δ^{18}O, this is not the case.

In the formation of the CO molecule, the binding oxygen atom could have three different sources, namely, the atmospheric oxygen, oxygen from plant water (H_2O) or another plant chemical. During the transition of freshly cut off to senescent, with no fresh water supply, the δ^{18}O value varied a lot. This could also indicate that plant liquids do play a role in the formation of CO.

The mean of the plant-emitted δ^{13}C(CO) was found to be 1,5 ‰ lower relative to the bulk value. This proves that the δ^{13}C value of plant-emitted CO can be different from the bulk composition. If modellers should want to use plant-emitted CO, the ^{13}C value of the bulk mass would likely be an estimation of the actual δ^{13}C value of CO.

As mentioned, Tarr et al. (1995) and Yonemura et al. (1999) reported senescent leaves could emit CO 1,3 to 9 times more per unit area of leaf and dead leaves were shown to emit more by an order of magnitude (Tarr et al., 1995; Yonemura et al., 1999). In the cut off test, the emissions increased by a factor ranging from 1,9 to 6,3, compared to the average living branch emission, which is in agreement. Although, the emission did not linearly increase as function of days. The emission rate on day 8 was found to be relatively very high, and there seems to be a peak in emission between day 4 and 15.

Further research on different plants is needed, preferentially in a more representative environment outdoor. If more tests are conducted, it is noted that the transition from live to dead leaves shows interesting variations and should be tested with a higher resolution. In arid regions where senescent leaves are abundant, the signature of senescent leaves will induce the highest impact on atmospheric CO composition, therefore, it would also be relevant to test if the signature of dead leaves will eventually remain constant, as indicated by the last three δ^{18}O) values in figure 12. Moreover, other plastics, which could be more CO-inert or/and stable compared to the FEP material, can be tested. The Polyfluor Plastics company offered to sent a test foil of polytetrafluoroethylene (PTFE), which possess a less complex chain of molecules, however, this foil was not received before the end of this research.

6 References

References

Alben, J., Deece, D., Bowne, S., Eisenstein, L., Frauenfelder, H., Good, D., and Marden, M. (1980). Isotope effect in molecular tunneling. *Physical Review Letters*, 44(April):1157–1160.

Austin, A. T. and Vivanco, L. (2006). Plant litter decomposition in a semi-arid ecosystem controlled by photodegradation. *Nature*, 442(7102):555–558.

Bergamaschi, P., Hein, R., Brenninkmeijer, C., and Crutzen, P. (2000a). Inverse modeling of the global CO cycle Inversioonf 13C/12C and 18O isotope ratios. *Journal of Geophysical Research*, 105:1929–1945.

Bergamaschi, P., Hein, R., Heimann, M., and Crutzen, P. J. (2000b). Inverse modeling of the global CO cycle 1. Inversion of CO mixing ratios. *Journal of Geophysical Research-Atmospheres*, 105(D2):1909–1927.

Bidwell, R. G. S. and Fraser, D. E. (1972). Carbon monoxide uptake and metabolism by leaves. *Canadian Journal of Botany*, 50(7):1435–1439.

Brandt, L. a., King, J. Y., Hobbie, S. E., Milchunas, D. G., and Sinsabaugh, R. L. (2010). The role of photodegradation in surface litter decomposition across a grassland ecosystem precipitation gradient. *Ecosystems*, 13(5):765–781.

Brenninkmeijer, C. (2009). Applications of stable isotope analysis to atmospheric trace gas budgets. *The European Physical Journal Conferences*, 1:137–148.

Brenninkmeijer, C., Röckmann, T., Bräunlich, M., Jöckel, P., and Bergamaschi, P. (1999). Review of progress in isotope studies of atmospheric carbon monoxide. *Chemosphere - Global Change Science*, 1:33–52.

Brenninkmeijer, C. a. M., Janssen, C., Kaiser, J., Röckmann, T., Rhee, T. S., and Assonov, S. S. (2003). Isotope Effects in the Chemistry of Atmospheric Trace Compounds. *Chemical Reviews*, 103:5125–5161.

Bruhn, D., Albert, K. R., Mikkelsen, T. N., and Ambus, P. (2013). UV-induced carbon monoxide emission from living vegetation. *Biogeosciences*, 10:7877–7882.

Conny, J. M. (1998). The isotopic characterization of carbon monoxide in the troposphere. *Atmospheric Environment*, 32(14-15):2669–2683.

Criss, R. (1999). *Principles of stable isotope distribution*. Oxford University Press.

Daniel, J. and Solomon, S. (1998). On the climate forcing of carbon monoxide. *Journal of Geophysical Research*, 103(D11).

Derendorp, L., Quist, J. B., Holzinger, R., and Röckmann, T. (2011). Emissions of H2 and CO from leaf litter of Sequoiadendron giganteum, and their dependence on UV radiation and temperature. *Atmospheric Environment*, 45(39):7520–7524.

Farquhar, Graham D. Ehleringer, J. and K.T., H. (1989). Carbon Isotope Discrimination and Photosynthesis. *Annual Review of Plant Physiology and Plant Molecular Biology*, 40:35.

Fishman, J. and Crutzen, P. J. (1978). The origin of ozone in the troposphere. *Nature*, 274(5674):855–858.

Giancoli, D. C. (2012). Hoofdstuk 40: moleculen en vaste stoffen. In *Natuurkunde: elektriciteit, magnetisme, optica en moderne fysica*, page 1453. Pearson Benelux, derde druk edition.

Huang, J., Mendoza, B., Daniel, J. S., Nielsen, C. J., Rotstayn, L., and Wild, O. (2013). Anthropogenic and Natural Radiative Forcing. *Climate Change 2013: The Physical Science Basis. Contribution of Working Group I to the Fifth Assessment Report of the Intergovernmental Panel on Climate Change*, pages 659–740.

Johnson, M. S., Feilberg, K. L., von Hessberg, P., and Nielsen, O. J. (2002). Isotopic processes in atmospheric chemistry. *Chemical Society reviews*, 31(6):313–323.

Khalil, M. and Rasmussen, R. (1994). Global decrease in atmospheric carbon monoxide concentration. *Nature*, 370.

Khalil, M. a. K. and Rasmussen, R. a. (1985). Causes of increasing atmospheric methane: Depletion of hydroxyl radicals and the rise of emissions. *Atmospheric Environment - Part A General Topics*, 19:397–407.

Kohn, M. J. (2010). Carbon isotope compositions of terrestrial C3 plants as indicators of (paleo)ecology and (paleo)climate. *Proceedings of the National Academy of Sciences of the United States of America*, 107(46):19691–19695.

Lee, H., Rahn, T., and Throop, H. (2012). An accounting of C-based trace gas release during abiotic plant litter degradation. *Global Change Biology*, 18:1185–1195.

Lu, Y. and Khalil, M. (1993). the Effects of Feedbacks and Reservoirs Oh + Co ˜ H + Co ˜. *Chermosphere*, 26(1989):641–655.

Manning, M. R., Brenninkmeijer, C. a. M., and Allan, W. (1997). Atmospheric carbon monoxide budget of the southern hemisphere: Implications of 13 C/ 12 C measurements. *Journal of Geophysical Research*, 102(D9):10673.

Park, K., Emmons, L., Wang, Z., and Mak, J. (2015). Joint Application of Concentration and δ18O to Investigate the Global Atmospheric CO Budget. *Atmosphere*, 6(5):547–578.

Park, K. H. (2010). *Joint Application of Concentration and Isotope Ratios to Investigate the Global Atmospheric Carbon Monoxide Budget: An Inverse Modeling Approach*. PhD thesis, Stony Brook University.

Pathirana, S., van der Veen, C., M.E., P., and Rockman, T. (2015). An analytical system for studying the stable isotopes of carbon monoxide using continuous flow-isotope ratio mass spectrometry (CF-IRMS). *Atmospheric Measurement Techniques Discussions*, 8:1–32.

Peterson, B. J. and Fry, B. (1987). Stable isotopes in ecosystem studies. *Annual Review of Ecology and Systematics*, 18(1987):293–320.

Prinn, R. G. (2003). The Cleansing Capacity of the at mosphere. *Annual Review of Environment and Resources*, 28(1):29–57.

Schade, G. W. and Crutzen, P. J. (1999). CO emissions from degrading plant matter (I). Measurements. *Tellus, Series B: Chemical and Physical Meteorology*, 51(5):909–918.

Shindell, D. T., Faluvegi, G., Koch, D. M., Schmidt, G. a., Unger, N., and Bauer, S. E. (2009). Forcing to Emissions. *Interactions*, 326(x):716–718.

Smiley, W. (1949). Note on reagent for oxidation of carbon monoxide. *Nuclear Science*.

Stevens, C., Krout, L., and Venters, A. (1972). The isotopic composition of atmospheric carbon monoxide. *Earth and Plantery Science Letters*, 16(2):147 – 165.

Stevens, C. and Wagner, A. (1989). The role of isotope fractionation effects in atmospheric chemistry. *Zeitschrift Fur Natorfoschung. A, A Journal of physical science*, 44a:376–384.

Tarr, M. a., Miller, W. L., and Zepp, R. G. (1995). Direct carbon monoxide photoproduction from plant matter. *Journal of Geophysical Research*, 100:11403.

Thompson, A. M. (1992). The Oxidizing Capacity of the Earth's Atmosphere: Probable Past and Future Changes. *Science*, 256(5060):1157–1165.

van Asperen, H., Warneke, T., Sabbatini, S., Nicolini, G., Papale, D., and Notholt, J. (2015). The role of photo- and thermal degradation for CO2 and CO fluxes in an arid ecosystem. *Biogeosciences Discussions*, 12:2429–2457.

Wang, C. and Prinn, R. G. (1999). Impact of emissions, chemistry and climate on atmospheric carbon monoxide: 100-yr predictions from a global chemistry–climate model. *Chemosphere - Global Change Science*, 1(1-3):73–81.

Wang, Z., Chappellaz, J., Martinerie, P., Park, K., Petrenko, V., Witrant, E., Emmons, L. K., Blunier, T., Brenninkmeijer, C. a. M., and Mak, J. E. (2012). The isotopic record of Northern Hemisphere atmospheric carbon monoxide since 1950: Implications for the CO budget. *Atmospheric Chemistry and Physics*, 12(10):4365–4377.

Yonemura, S., Morokuma, M., Kawashima, S., and Tsuruta, H. (1999). Carbon monoxide photoproduction from rice and maize leaves. *Atmospheric Environment*, 33:2915–2920.

Zeebe, R. and Wolf-Gladrow, D. (2001). Stable Isotope Fractionation. In *CO2 in Seawater: Equilibrium, Kinetics, Isotopes: Equilibrium, Kinetics, Isotopes*, chapter 3: Stable, pages 141 – 250. Elsevier, 1st editio edition.

Appendix A

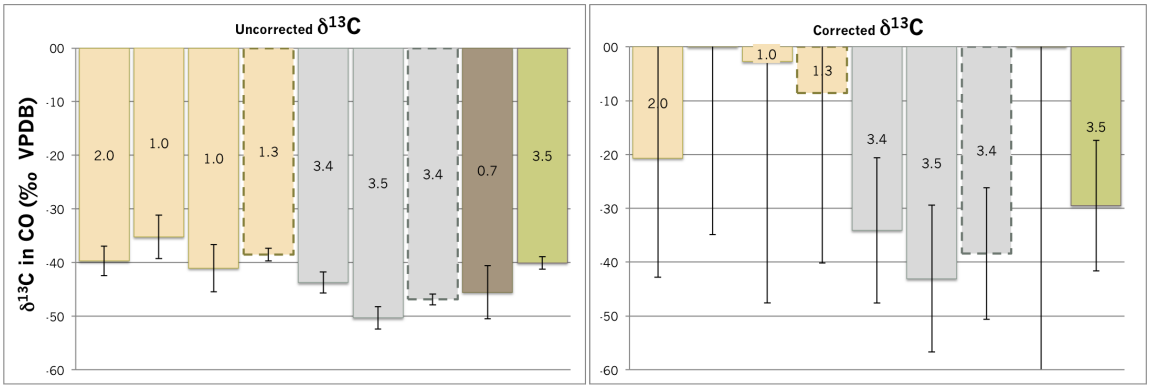

Figure 14: Uncorrected and corrected δ^{13}C values of the four living leaf tests, test 1 (left) to 4 (right), each having their own colour, are presented. The dotted bars are the δ values calculated over all corresponding datapoints of that test, the numbers inside the bars give the ratio plant/blank. In the left graph, the δ^{13}C was calculated as described in section 3.5. The emission of the bags and its corresponding strong depletion in ^{13}C, caused need for correction, as discussed in section 4.1. If the emission of the plant was low, a small over- or understatement of the emission or δ value, will lead to a high impact on the corrected plant-emitted δ value. When looking at the corrected values, the correction seems to be substantially overcompensating. Until now, it remains unclear why the uncorrected values with a low plant/blank ratio, were not closer to the δ value of the bags (table 2) and whether the origin of this particular result is caused by an overestimated correction (faulty bag signature and/or emission) or the uncorrected values are wrong and should be more depleted.

Appendix B

(see next page)

Table 4: The results of all measurements on blank bag CO emission, by either the RGA corresponding to number 1 or the GC-IRMS corresponding to number 0. The time exposed did not show a clear correlation to the amount of emission.

Date	Bag	Corresponding to test	RGA 1 GC-IRMS 0	time exposed	ppb/hr
25-Mar	2	1	1	1,00	4,0
25-Mar	4	1	1	1,00	6,0
26-Mar	2	2	1	1,00	12,0
26-Mar	4	2	1	1,00	5,0
27-Mar	2	4	1	1,00	5,0
27-Mar	3	4	1	1,00	8,0
27-Mar	5	4	1	1,00	5,5
31-Mar	2	5	1	1,58	11,4
31-Mar	3	5	1	1,58	9,2
31-Mar	5	5	1	1,58	12,0
01-Apr	0	6	1	1,50	15,3
01-Apr	0	6	1	1,50	6,9
01-Apr	4	6	1	1,50	7,3
02-Apr	2	7	1	1,53	5,9
02-Apr	4	7	1	1,53	13,1
02-Apr	5	7	1	3,18	9,4
02-Apr	5	7	0	3,18	6,6
14-Apr	2	-	1	4,27	8,9
14-Apr	2	-	0	4,27	6,3
14-Apr	6	-	0	5,13	5,3
14-Apr	3	-	1	5,13	7,8
14-Apr	3	-	0	5,13	6,2
15-Apr	3	8	1	2,67	4,5
15-Apr	4	8	1	2,67	2,6
15-Apr	6	8	1	2,67	4,5
16-Apr	2	9	1	3,33	2,4
16-Apr	4	9	1	3,33	4,5
16-Apr	5	9	1	3,33	3,9
17-Apr	2	10	1	3,00	5,7
17-Apr	3	10	1	3,00	4,0
17-Apr	4	10	1	3,00	3,7
17-Apr	5	10	1	3,00	10,0
20-Apr	3	11	1	3,00	4,3
20-Apr	4	11	1	3,00	2,0
20-Apr	5	11	1	3,00	4,7
21-Apr	4	12	1	3,00	3,7
21-Apr	5	12	1	3,00	3,3
28-Apr	5	13	1	1,72	8,1
28-Apr	6	13	1	1,72	5,2

Appendix C

(see next page)

Table 5: The data obtained from all experiments, NC presents the values not corrected for bag emission and Corr. is short for the corrected values. The number after the cut off type experiment, represents the number of days after the branch was cut.

Type	Test	Blank CO [ppb]	Plant CO [ppb]	NC $\delta^{13}C$	$\sigma^{13}C$	NC $\delta^{18}O$	$\sigma^{18}O$	Corr. $\delta^{13}C$	$\sigma^{13}C$	Corr. $\delta^{18}O$	$\sigma^{18}O$
Living	1	7	12	-39,8	2,7	26,2	2,3	-20,7	22,1	34,6	10,9
Living	1	7	6	-35,2	4,0	26,3	2,7	7,9	42,8	43,2	25,7
Living	1	7	6	-41,0	4,4	30,6	3,8	-2,7	44,8	53,5	33,2
Average	1	20	23	-38,5	1,2	31,5	1,1	-8,6	31,6	48,8	8,7
Living	2	7	20	-43,8	1,9	31,8	1,7	-34,1	13,5	38,5	6,9
Living	2	7	21	-50,3	2,1	35,0	1,8	-43,1	13,6	42,4	7,3
Average	2	13	41	-46,9	1,0	32,8	0,9	-38,4	12,2	39,6	3,8
Living	3	7	4	-45,6	4,9	27,8	4,0	2,4	65,2	56,2	50,1
Living	4	10	31	-40,1	1,2	31,6	1,0	-29,5	12,2	38,0	4,6
Stressed	5	5	7	-32,58	4,01	36,90	3,85	-1,73	28,84	56,23	29,24
Stressed	5	5	17	-40,14	2,29	27,61	1,93	-30,60	12,45	32,27	6,85
Average	5	10	24	-37,77	1,47	30,52	1,27	-22,96	15,75	38,49	6,10
Stressed	6	10	85	-45,43	0,56	6,29	0,40	-42,19	4,60	6,15	1,18
Stressed	7	10	395	-35,25	0,19	15,45	0,17	-34,28	1,00	15,65	0,61
Cut-off light (0)	8	10	-21	-52,1	5,0	-188,1	12,6	-62,2	15,9	-93,4	17,4
Cut-off light (0)	8	10	69	-36,1	0,7	12,7	0,5	-30,7	4,1	12,9	1,2
Average (0)	8	20	48	-35,3	0,8	21,9	0,4	-19,6	6,8	26,3	3,0
Cut-off light (1)	10	10	73	-36,0	0,6	-5,4	0,5	-30,6	4,1	-7,8	1,1
Cut-off dark (1)	10	10	0	-25,3	1,2	-40,7	1,2	-35,0	5,7	-30,3	2,6
Cut-off light (4)	9	9	73	-40,1	0,6	4,7	0,4	-36,0	3,9	3,8	1,0
Cut-off light (4)	9	9	68	-192,3	16,2	243,0	19,9	9050,3	251799,1	-17756,2	493990,2
Average (4)	9	18	-49	-48,5	0,6	17,8	0,3	-42,3	4,6	19,4	1,8
Cut-off light (5)	11	10	82	-40,3	0,5	-3,8	0,4	-36,3	3,5	-5,7	0,9
Cut-off dark (5)	11	10	30	-51,6	1,6	46,3	1,4	-44,4	10,1	58,0	6,9
Cut-off light (8)	12	26	227	-50,2	0,3	22,0	0,2	-47,5	1,3	23,2	0,5
Cut-off dark (8)	12	26	341	-45,6	0,3	19,3	0,3	-43,5	0,9	19,9	0,6
Cut-off light (12)	13	26	72	-44,5	0,5	23,4	0,4	-34,1	4,0	27,7	1,7
Cut-off dark (12)	13	26	177	-35,1	0,3	25,2	0,3	-29,5	1,6	27,2	1,0
Cut-off light (15)	14	10	67	-44,9	0,6	21,3	0,5	-40,6	4,4	22,7	1,5
Cut-off dark (15)	14	10	57	-39,1	0,8	20,1	0,7	-33,1	4,9	21,7	1,8